BBA - Biomembranes 1863 (2021) 183498

Contents lists available at ScienceDirect

BBA - Biomembranes

journal homepage: www.elsevier.com/locate/bbamem

Interaction of the antimicrobial peptide ΔM3 with the *Staphylococcus aureus* membrane and molecular models

Marcela Manrique-Moreno [a,*], Mario Suwalsky [b], Edwin Patiño-González [a], Estefanía Fandiño-Devia [a], Małgorzata Jemioła-Rzemińska [c,d], Kazimierz Strzałka [c,d]

[a] Faculty of Exact and Natural Sciences, University of Antioquia, Medellin, Colombia
[b] Facultad de Medicina, Universidad Católica de la Santísima Concepción, Concepción, Chile
[c] Faculty of Biochemistry, Biophysics and Biotechnology, Jagiellonian University, Krakow, Poland
[d] Malopolska Centre of Biotechnology, JagiellonianUniversity, Krakow, Poland

ARTICLE INFO

Keywords:
Staphylococcus aureus
Cationic antimicrobial peptide
Lipid bilayer
Peptide-membrane interactions

ABSTRACT

Staphylococcus aureus is one of the most pathogenic bacteria; infections with it are associated with significant morbidity and mortality in health care facilities. Antimicrobial peptides are a promising next generation antibiotic with great potential against bacterial infections. In this study, evidence is presented of the biological and biophysical properties of the novel synthetic peptide ΔM3. Its antimicrobial activity against the ATCC 25923 and methicillin-resistant *S. aureus* strains was evaluated. The results showed that ΔM3 has activity in the same μM range as vancomycin. Biophysical studies were performed with palmitoyloleoylphosphatidylglycerol and cardiolipin liposomes loaded with calcein and used to follow the lytic activity of the peptide by fluorescence spectroscopy. On the other hand, ΔM3 was induced to interact with molecular models of the erythrocyte membrane buil-up of dimiristoylphosphatidylcholine and dimyristoylphosphatidylethanolamine, representative lipids of the outer and inner monolayers of the human erythrocyte membrane, respectively. The capacity of ΔM3 to interact with the bacteria and erythrocyte model membranes was also evaluated by X-ray diffraction and differential scanning calorimetry. The morphological changes induced by the peptide to human erythrocytes were observed by scanning electron microscopy. Results with these techniques indicated that ΔM3 interacted with the inner monolayer of the erythrocyte membrane, which is rich in anionic lipids. Additionally, the cytotoxic effects of ΔM3 on red blood cells were evaluated by monitoring the hemoglobin release from erythrocytes. The results obtained from these different approaches showed ΔM3 to be a non-cytotoxic peptide with antibacterial activity.

1. Introduction

α-cationic antimicrobial peptides (α-cAMPs) participate in the first line of defense against the attack of pathogens [1,2]. Most of these peptides are formed by about 50 residues, have a net positive charge, and are amphipathic. The initial binding of α-cAMPs to bacterial membranes is mediated through electrostatic interactions between the cationic residues on the peptide and anionic lipids of the membrane target. A promising feature of α-cAMPs in comparison with conventional antibiotics is that α-cAMPs execute their biological activity via a non-specific mechanism, mainly targeting bacterial cell membranes, which makes it less likely that bacteria will develop resistance [3]. This promising property is important due to the growing number of *Staphylococcus aureus* (*S. aureus*) infections that have been reported worldwide, increasing morbidity and putting a strain on health services. *S. aureus* is widely recognized as being one of the leading pathogenic bacteria involved in healthcare-associated infections [4]. It is normally found in a harmless form in the nose and the skin of approximately 30% of healthy adults [5]. However, when the bacteria invades the body, it causes several diseases such as bacteremia, pneumonia, joint infections, and

Abbreviations: MLV, multilamellar vesicles; DSC, differential scanning calorimetry; RBC, red blood cells; RBCS, red blood cell suspension; MIC, minimum inhibitory concentration; SEM, scanning electron microscopy; LUV, large unilamellar vesicles; POPG, palmitoyloleoylphosphatidylglycerol; DMPC, dimyristoylphosphatidylcholine; DMPE, dimyristoylphosphatidylethanolamine; CL, cardiolipin; MRSA, methicillin-resistant *Staphylococcus aureus*.

* Corresponding author.
E-mail address: marcela.manrique@udea.edu.co (M. Manrique-Moreno).

https://doi.org/10.1016/j.bbamem.2020.183498
Received 8 August 2020; Received in revised form 22 September 2020; Accepted 12 October 2020
Available online 4 November 2020

osteomyelitis [4]. Nosocomial infections due to methicillin-resistant *Staphylococcus aureus* (MRSA) have become a major cause of morbidity and mortality in many care units [6,7]. Several mechanisms of multidrug resistance have been described for *S. aureus*, including membrane phospholipid modifications that are triggered in response to the growth phase [8–10], or medium stressors such as changes in pH, osmotic stress, the presence of organic solvents and high saline concentrations. These adaptive responses are related to the induction of resistance to membrane-active antibiotics [11]. Therefore, efforts to design and evaluate potential antibiotics against *S. aureus* are necessary.

In previous studies we focused on designing and evaluating synthetic peptides derived from cecropin D-like, a 39-residue peptide neutral at pH 7.4, active against Gram-negative and Gram-positive bacteria, as well as filamentous fungus *A. niger* [12]. After some modifications to defined residues it became ΔM2, a peptide of the same size, with a charge of +9 at physiological pH. The increase in charge in the polar face of the structure caused a substantial increase in antimicrobial activity, reaching a minimum inhibitory concentration (MIC) of 5 μM in *S. aureus* [13]. After further modifications of ΔM2, the peptide ΔM3 was obtained. This is a 20-residue α-cAMP, corresponding to the N-terminal fragment of ΔM2, which at physiological pH has a charge of +8.

Understanding the molecular basis of the antimicrobial and cytotoxic properties of peptides is an important step in designing new molecules as potential therapeutic agents. Biophysical studies on model membranes give valuable insights into the peptide mechanism of action; for this reason, this work presents the biophysical evaluation of the interaction of ΔM3 with representative phospholipids of the bacterial membrane. In order to understand the activity of the peptide, palmitoyloleoylphosphatidylglycerol (POPG) and cardiolipin (CL) were selected as representative lipids of *S. aureus* membrane. These two lipids were loaded with calcein and used to follow the lytic activity of the peptide by fluorescence spectroscopy [14]. On the other hand, ΔM3 was induced to interact with molecular models of the human erythrocyte membrane. Human erythrocytes were chosen since they have only one membrane and no internal organelles, making them an ideal cell system for studying basic peptide-membrane interactions. Dimiristoylphosphatidylcholine (DMPC) and dimyristoylphosphatidylethanolamine (DMPE) were used as the representative lipids of the outer and inner monolayers of the human erythrocyte membrane, respectively. The capacity of ΔM3 to interact with the bacteria and erythrocyte model membranes was also evaluated by X-ray diffraction and differential scanning calorimetry (DSC). The morphological changes induced by the interaction of the peptide with the human erythrocyte membrane were observed by scanning electron microscopy (SEM). Additionally, the cytotoxic effects of the peptide on red blood cells were evaluated by monitoring the hemoglobin release from erythrocyte cell suspensions, and quantified by spectrophotometry. The results obtained from these different approaches showed ΔM3 to be a non-cytotoxic peptide with antibacterial activity.

2. Material and methods

2.1. Reagents

1-,2-dimyristoyl-*sn*-glycero-3-phosphoglycerol sodium salt (DMPG, Lot 140PG-167), 1,2-dimyristoyl-*sn*-glycero-3-phosphocholine (DMPC, Lot 140PC-268), 1,2-dimyristoyl-sn-glycero-3-phosphoethanolamine (DMPE, Lot 140PE-67) and 1-palmitoyl-2-oleoyl-*sn*-glycerol-3-phosphoglycerol sodium salt (POPG, Lot 160-181PG-135) were from Avanti Polar Lipids (Alabaster, AL, USA) Fig. S1. Tetraoleoylcardiolipin from heart bovine (CL, Lot SLBL8560V), 3,3-bis[*N*,*N*-bis(carboxymethyl)-aminomethyl]fluorescein (Calcein), N-2-hydroxyethylpiperazine-N′-2-ethanesulfonic acid (HEPES) and Sephadex G50-fine were from Sigma-Aldrich (St. Louis, MO, USA). Vancomycin was from Amresco (Solon, OH, USA), ΔM2 (RNFFKRIRRAGKRIRKAIISAAPAVETLAQAQKIIKGGD, Lot 88771380003/PE2076) and ΔM3 (NFFKRIRRAGKRIRKAIISA, Lot 7215960005/PE6969) were synthesized according to the sequence by the solid-phase method and purchased from GenScript (Piscataway-Township, NJ, USA). The purity of the peptide (higher than 95%) was determined by analytical HPLC, and the molecular weight was confirmed with MALDI-TOF mass spectrometry. All other reagents of analytical grade were from Sigma-Aldrich.

2.2. Prediction of the peptide structure

A prediction of the 3D structure of ΔM3 peptide was generated using two types of software: I-TASSER generated the atomic model through the identification of structural templates from the PDB using LOMETS; the structure was predicted by multiple threading alignments and iterative structural assembly simulation (https://zhanglab.ccmb.med.umich.edu/I-TASSER/). The atomic model was refined using ModRefiner to obtain a peptide structure closer to its native form (https://zhanglab.ccmb.med.umich.edu/ModRefiner/) [15].

2.3. Culture conditions and antimicrobial activity

Strains used in the experiments were *S. aureus* ATCC 22923 and MRSA; the latter a donation from the Basic and Applied Microbiology Group (MICROBA) of the University of Antioquia. MRSA was phenotypically and genotypically characterized as resistant to β-lactamic antibiotics and susceptible to fifth-generation cephalosporins (ceftaroline and ceftobiprole). Strains were kept at −70 °C in 10% glycerol and grown in Müller Hinton (MH). The determination of the minimum inhibitory concentration (MIC) was performed according to Wiegand et al. [16], and to the Clinical & Laboratory Standard Institute (CLSI). Strains were grown at 37 °C, shaked at 200 rpm for 12–14 h, and the culture of each strain was set at 0.5 in McFarland scale (10^8 CFU ml^{-1}). Next, 50 μl aliquots of these cell suspensions were mixed with 50 μl ΔM3 solution at different concentrations (0.625 to 60 μM) in a 96-well microplate, and incubated at 37 °C in an orbital shaker (200 rpm for 8 h). The growth kinetics of each microorganism were determined by triplicate in an Elisa lector (Bio-Rad, CA, USA), measuring the absorbance at 595 nm. Vancomycin (6 μg/ml or 4 μM) and PBS were used as positive and negative controls, respectively.

2.4. Hemolytic activity

Hemolytic activity was performed according to Spaller et al. [17]. Erythrocytes were isolated from fresh human peripheral blood; washed three times with PBS (10 mM, pH 7.4 and 150 mM NaCl) by centrifugation for 5 min at 400 *g* and resuspended in PBS to obtain an approximately constant 5×10^5 cells for each test. ΔM3 at different concentrations (0.625 to 60 μM) was added to human erythrocytes in PBS and incubated at 37 °C for 1 h. The mixtures were then centrifuged at 400 *g* for 5 min. Aliquots of the supernatant were transferred to 96-well plates. Hemolysis was measured by absorbance at 540 nm in a Multiskan Go (Thermo, Waltham, USA). PBS and melittin (5 μM) were used as negative and positive controls, respectively according to Oddo and Hansen [18]. The percentage of hemolysis was calculated according to Eq. (1):

$$\text{Hemolysis } (\%) = \frac{(\text{Abs in the peptide solution} - \text{Abs in PBS})}{(\text{Abs in Melittin} - \text{Abs in PBS})} \times 100 \quad (1)$$

2.5. Calcein permeability assay

Two lipid systems were prepared for the calcein leakage experiments, one of pure POPG and another of POPG:CL (80:20). Experiments were performed following the basic steps described by Maherani et al. [19]. Lipid films were prepared by dissolving 4 mg per ml of lipid (POPG or POPG:CL) in chloroform. The solvent was evaporated under a stream of nitrogen and the samples were kept under a vacuum for at least 1 h to ensure complete solvent removal. The lipid films were rehydrated in a

buffer (20 mM HEPES, 145 mM NaCl at pH 7.4) containing 50 mM calcein, and multilamellar vesicles (MLV) were formed after vortexing these for 7 min. The calcein buffer was prepared as follows: 1.09 g of calcein was dissolved in 5 ml of 1 M NaOH. After the calcein was fully dissolved, 2.5 ml of buffer (20 mM HEPES, pH 7.4) was added, together with 5 ml of MilliQ water (Millipore, Bedford, MA). The solution was then pH-adjusted to 7.4 with 1 M HCl dropwise while being stirred constantly to avoid precipitation. MilliQ water was then added to bring the calcein buffer to a final volume of 25 ml and calcein concentration of 50 mM. The MLV were subjected to 5 cycles of freezing and thawing in liquid nitrogen to increase the yield of calcein encapsulation.

Large unilamellar vesicles (LUV) were obtained using a mini-extruder from Avanti Polar Lipids (Alabaster, AL, USA) with a polycarbonate filter of 200 nm. The dye-containing vesicles were separated from non-entrapped calcein using a size exclusion chromatographic column Sephadex G50 Fine (10 × 150 mm), eluted with HEPES buffer that did not contain calcein. Kinetic experiments were carried out as follows: 50 μl of the liposome suspension of each lipid system was added to 1950 μl of buffer (10 mM HEPES, 143.2 mM NaCl, pH 7.4) and incubated at 37 °C for 5 min while being stirred. Fluorescence intensity was measured with a Fluomax-3 stirring cell spectrofluorometer from HORIBA JobinYvon (Edison, NJ) at excitation and emission wavelengths of 480 and 520 nm, respectively. The stability of the liposomes was monitored for 3 min before the peptide was added. The kinetics of calcein release after the addition of the peptide was recorded for 10 min; a complete release (100%) was achieved by the addition of TritonX-100 to a final concentration of 0.05%. The apparent percentage of calcein release (normalized membrane leakage) was calculated according to Eq. (2):

$$L_T = \frac{F - F_0}{F_{100} - F_0} \times 100 \quad (2)$$

in which F and F_{100} represent the fluorescence intensity prior to and after the addition of the detergent, respectively and F_0 represents the fluorescence of the intact vesicles. The experiments were performed in triplicate on independent samples of calcein-loaded liposomes. The results are presented as the average with their standard deviations.

2.6. X-Ray diffraction of DMPC and DMPE multilayers

Multilayers were prepared using the lipid hydration technique. About 2 mg of each phospholipid was mixed in Eppendorf tubes with 200 μl of (a) distilled water and (b) appropriate amounts of ΔM3 in a range of concentrations (1 to 300 μM). The specimens were incubated for 30 min at 37 °C and 60 °C with DMPC and DMPE, respectively. The samples were then transferred to 1.5 mm diameter special glass capillaries (Glas-Technik&Konstruktion, Berlin, Germany), centrifuged for 45 min at 1462 *g* and X-ray diffracted. Specimen-to-film distances were 8 and 14 cm, standardized by sprinkling calcite powder on the capillary surface. Ni-filtered CuKα radiation was obtained from a Bruker Kristalloflex 760 (Karlsruhe, Germany) X-ray generator. The relative reflection intensities were collected in an MBraun PSD-50 M linear position-sensitive detector system (Garching, Germany); no correction factors were applied. The experiments were performed at 18 ± 1 °C, which is below the main phase transition temperature of both DMPC and DMPE. Higher temperatures would have induced transitions to more fluid phases making the detection of structural changes harder. Each experiment was performed three independent times.

2.7. Differential scanning calorimetry (DSC) of DMPC and DMPG MLV

Appropriate amounts of DMPG or DMPC were weighed in order to obtain a 1 mM final phospholipid concentration. Lipids were dissolved in pure chloroform in a glass test tube, the solvent was dried under a stream of nitrogen and the traces were removed by keeping the samples under reduced pressure (about 13.3 Pa) for 30 min. Dried lipids were hydrated in water for DMPC and buffer (10 mM HEPES, 500 mM NaCl, 1 mM EDTA, pH 7.4) for DMPG. MLV were formed by vortexing the samples above the main phase transition temperature of the lipids for at least 15 min. ΔM3 stock solution was prepared in buffer (10 mM HEPES, pH 7.4) and added in different volumes to the liposome suspensions depending on the molar ratio of the mixture. DSC measurements were performed in a Nano DSC device (TA Instruments, New Castle, USA). The sample cell was filled with 400 μl of MLV suspension; a reference of an equal volume of buffer was used. The cells were sealed and equilibrated for about 10 min at the starting temperature. Heating/cooling rates were 1 °C per minute and the scans were recorded within a range of 5 °C to 40 °C. Heating scans were carried out first. The reference scan was subtracted from the sample scan. Each data set was analyzed and the values of transition temperatures were calculated using a software package supplied by TA Instruments. At least three independently prepared samples were measured to check the reproducibility of the DSC experiments. The accuracy was ±0.1 °C for the main phase transition temperature and ±1 kJ mol^{-1} for the main phase transition enthalpy.

2.8. Scanning electron microscopy (SEM) observations of human erythrocytes

Blood was obtained from a healthy human male donor not receiving any pharmacological treatment. Blood samples (0.1 ml) were obtained by puncture of the ear lobule and drawn into an Eppendorf tube containing 10 μl of heparin (5000 UI/ml) in 0.9 ml of saline solution (NaCl 0.9%, pH 7.4). The sample was centrifuged (1000 rpm for 10 min); the supernatant was discarded and replaced by the same volume of saline solution; the whole process was repeated three times. The red blood cells were suspended in 0.9 ml of saline solution, and fractions of this stock of red blood cell suspension (RBCS) and saline solution were placed in Eppendorf tubes to prepare: (a) the control, by mixing 100 μl of saline solution plus 100 μl RBCS, and (b) a range of concentrations of ΔM3 by mixing 100 μl of RBCS with a known volume of ΔM3 stock solution. All samples were then incubated for one h at 37 °C. After the incubation, samples were centrifuged (1000 rpm for 10 min) and the supernatant was discarded. They were fixed overnight at 4 °C by adding 500 μl of 2.5% glutaraldehyde to each sample. The fixed samples were washed with distilled water, placed over Al glass cover stubs, air-dried at 37 °C for 30 min to 1 h, and gold-coated for 3 min at 13.3 Pa in a sputtering device (Edwards S150, Sussex, England). The resulting specimens were scanned in a Jeol SEM (JSM 6380 LB, Japan).

3. Results

3.1. Prediction of the 3D structure of ΔM3

ΔM3 is a synthetic α-cAMP of 20 residues with a + 8 charge at physiological conditions. This fragment contains almost all amino acids related to the global charge of the parent peptide ΔM2, a 39 residue peptide with a + 9 charge at pH 7.4. ΔM2 was previously designed and synthesized by us, and showed high selectivity toward anionic bacterial membranes [13]. Fig. 1A presents the helical wheel projection of the ΔM3 peptide; it shows an amphipathic structure with two faces, one conserving the hydrophobic residues and the other forming a polar surface. α-cAMPs are usually unfolded in aqueous environments, but generally fold during their interaction with membranes [20]. According to the I-TASSER results, the prediction of the secondary structure of ΔM3 shows a single α-helix (Fig. 1B).

3.2. Antimicrobial and hemolytic activities of ΔM3

Using the broth microdilution assay, the antimicrobial activity of ΔM3 against *S. aureus* ATCC 25923 and MRSA strains was determined. The results showed that ΔM3 was active, with an MIC of 5 and 7.5 μM

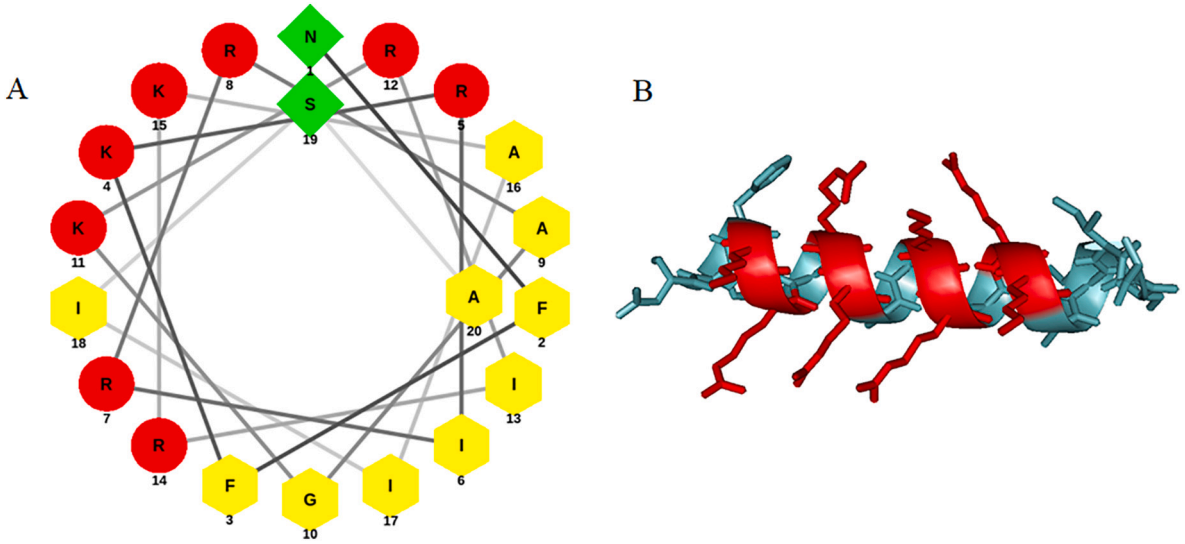

Fig. 1. Prediction of ΔM3 helical structure. (A) helical-wheel projection of ΔM3 peptide. Basic residues are presented as red circles, non-polar residues as yellow hexagons, and polar uncharged residues as green squares. (B) Predicted α-helical structure of the ΔM3 peptide; positive charged residues are highlighted in red. (For interpretation of the references to colour in this figure legend, the reader is referred to the web version of this article.)

against *S. aureus* ATCC 25923 and MRSA, respectively. Vancomycin was used as a positive control, with an MIC of 4 μM, equivalent to 6 μg/ml according to the Clinical & Laboratory Standards Institute guidelines [21]. Previously we had performed the same procedure in order to evaluate the antimicrobial activity of ΔM2 against *S. aureus* reaching a MIC of 5 μM [13]. The hemolytic experiments were performed by incubating suspensions of human red blood cells with serial dilutions of the ΔM2 and ΔM3 peptides, the results are presented in Fig. 2. At low concentrations, equivalent to the MIC (5 μM) the hemolytic activity reached a maximum of approximately 0.4% for both peptides. Even at a concentration two times that of MIC there was no significant differences in the hemolytic activity of the peptides. At concentrations three or four times higher, ΔM2 induced 0.6% and ΔM3 induced just 5% of RBC hemolysis. As a comparison, the peptide melittin that binds spontaneously to biological membranes and causes a significant membrane disruption, at 5 μM induced a 98% of hemolysis [22].

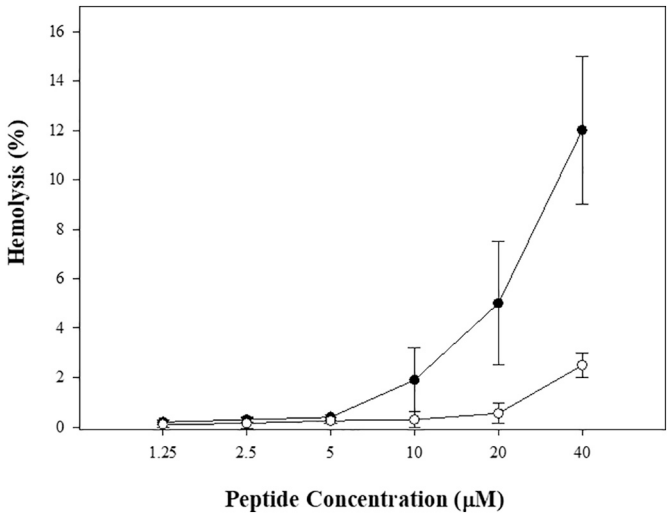

Fig. 2. ΔM3 (●) and ΔM2 (○) hemolytic activity on human erythrocytes. The values represent the average mean ± S.D. (n = 3). Melittin and PBS were used as positive and negative controls, respectively.

3.3. Calcein leakage experiments

The ability of ΔM3 to induce leakage on synthetic model membranes was studied on POPG and POPG:CL (80:20). These lipids were selected due to be the predominant constituents of the *S. aureus* membrane [23]. The results of the kinetic experiment of ΔM3 added to the calcein-loaded LUV at 37 °C are presented in Fig. 3A. They showed that the liposomes were stable during the incubation period, and after 3 min with stirring there was no leakage caused by the experimental conditions. After the incubation, ΔM3 was added and calcein release was immediately observed (black arrow). Kinetics of the calcein release were recorded for 10 min; during this period, the effect of the peptide on the liposomes reached its highest activity, after which the disrupting effect was stable and did not increase with time. The red arrow in Fig. 3A represents the moment when Triton X-100 was added to the liposome suspension and inducing the total leakage of the calcein-entrapped vesicles. Fig. 3B shows the results obtained after ΔM3 was added in different concentrations to the POPG and POPG:CL (80:20) lipid systems. The addition of ΔM3 in increasing concentrations to the dye-containing LUV induced calcein release in both systems in a concentration-dependent manner. However, the disrupting effect of ΔM3 was higher in POPG vesicles; at the lowest 1% assayed ΔM3 molar percentage the leakage was 7.2%, compared to the 3.4% in POPG:CL liposomes. At 3% ΔM3 concentration the leakage was 38.5% for POPG and 10.6% for POPG:CL liposomes.

3.4. X-Ray diffraction experiments on DMPC and DMPE multibilayers

In order to understand the molecular interactions of ΔM3 with cell membranes, different biophysical experiments were carried out with model membranes and human red blood cells. The interaction of ΔM3 with DMPC and DMPE multibilayers was determined by X-ray diffraction. These lipids represent phospholipid classes that are present in the outer and inner monolayers of eukaryotic and red cell membranes, respectively. It can be observed in Fig. 4A that water altered the DMPC structure. Its bilayer repeat (bilayer width plus the width of the water layer between bilayers) increased from about 55 Å in its dry crystalline form to 64.5 Å when it was immersed in an excess of water [24], and its low-angle reflections (indicated as (a) in the figure), which correspond to DMPC polar terminal group distance were reduced to only the first two orders of the bilayer repeat. On the other hand, only one strong

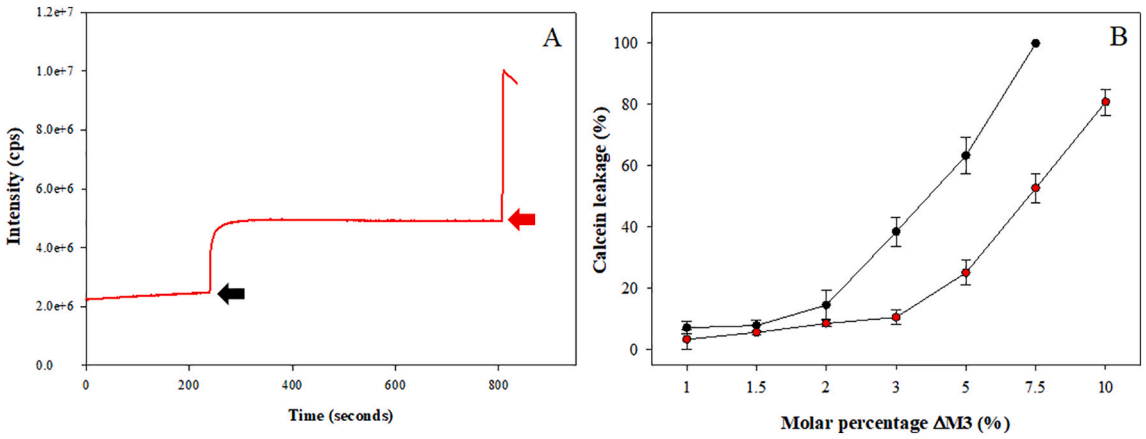

Fig. 3. A) Time-course of calcein release from liposomes after the addition of 2.5% of the ΔM3 peptide. LUV were incubated for approximately 4 min at pH 7.4 and 37 °C with stirring; after that period the peptide was added (black arrow). The complete release of the dye (100%), due to the total leakage of the vesicles was achieved by the addition of Triton X-100 at 0.1% (red arrow). B) Membrane permeabilization effect induced by ΔM3 on calcein-containing POPG (●) and POPG:CL 80:20 vesicles (●). After the peptide addition, liposomes were incubated approximately for 10 min. 100% calcein release was obtained using Triton X-100. (For interpretation of the references to colour in this figure legend, the reader is referred to the web version of this article.)

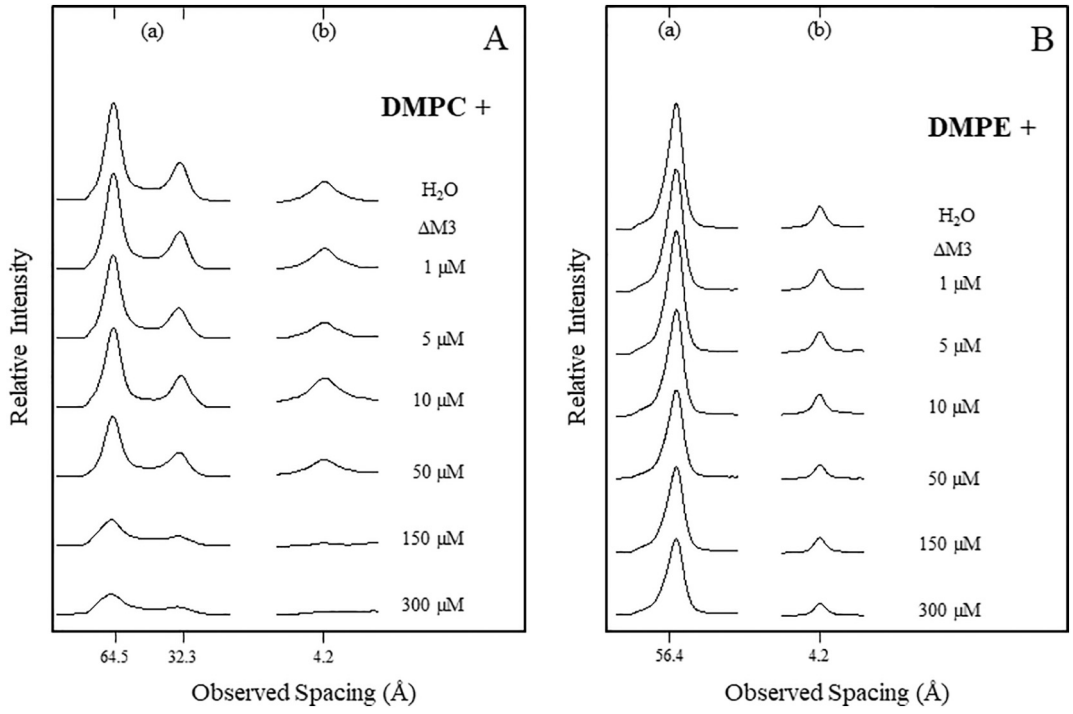

Fig. 4. X-ray diffraction patterns of A) dimyristoylphosphatidylcholine (DMPC) and B) dimyristoylphosphatidylethanolamine (DMPE) in water and with different concentrations of ΔM3; (a) small-angle and (b) wide-angle reflections.

reflection of 4.2 Å appeared in the wide-angle region (b), which corresponds to the average distance between fully extended acyl chains organized with rotational disorder in hexagonal packing. Fig. 4A also shows the diffraction patterns of DMPC multilayers incubated with different concentrations of ΔM3. After exposure to 5 μM and higher ΔM3 concentrations DMPC bilayers underwent a regular and monotonic reduction of their small and wide-angle reflection intensities, indicated as (a) and (b) in the figure, respectively. With 10 μM, the reduction in the intensities was 3%, with a concentration that was equivalent to twice the MIC value obtained in the previous results. With higher ΔM3 concentrations, the reduction in the reflection intensities was more evident; in fact, 300 μM ΔM3 induced a 70% intensity decrease, reflecting a marked disturbance of DMPC bilayer structure. The results of the X-ray diffraction patterns of DMPE bilayers incubated in water and ΔM3 solutions are shown in Fig. 4B. As reported elsewhere, water did not significantly affect the bilayer structure of DMPE [24]. However, after heating to 60 °C and cooling to room temperature (ca. 18 °C) DMPE was properly hydrated reaching a fluid state as its X-ray reflections were reduced to one of 56.4 Å and another of 4.2 Å in the low- and wide-angle regions, respectively. The diffraction patterns also showed that increasing concentrations of ΔM3 caused a weakening in DMPE reflection intensities, albeit less marked compared with that observed in DMPC. In fact, after incubation with 50 μM ΔM3, only a 15% reduction of the reflection intensities was attained, while with 300 μM the reduction reached 35%, half the percentage observed in DMPC.

3.5. Differential scanning calorimetry (DSC) of DMPC and DMPG MLV

Calorimetric experiments were performed in order to determine the effect of the ΔM3 peptide on the thermotropic properties of DMPC and DMPG MLV. DMPC is the most abundant lipid in the outer monolayer of the human erythrocyte membrane, and phosphatidylglycerol (PG) is the predominant phospholipid constituent of the *S. aureus* membrane, present in an 80% [23,25,26]. The single DMPC thermogram (Fig. 5A) shows two endothermic peaks; the small one at a lower temperature (15.18 °C) corresponds to the transition from gel phase ($L_{\beta'}$) into the ripple phase ($P_{\beta'}$), the so-called pretransition, and the large peak at a higher temperature (24.01 °C) corresponds to the main phase transition with a $\Delta H = 23$ kJ mol^{-1}. The $P_{\beta'}$ is one of the gel phases that occurs due to structural constraints between the packing characteristics of the two acyl chains and the headgroups [27]. Fig. 5A shows that the addition of the peptide had almost no effect on DMPC phase transition. Interestingly, the metastable ripple phase was still observed even at the highest assayed peptide concentration (5%). Fig. 5B presents the thermograms during heating of pure DMPG and DMPG in the presence of ΔM3. Fully hydrated DMPG liposomes in buffer showed a pretransition at 15 °C, followed by the main transition at 23.7 °C with an enthalpy of 31.9 kJ mol^{-1}. The effect of the peptide with the charged lipid was different from the zwitterionic DMPC. At the lowest assayed concentrations (0.1 and 1%), there was a significant decrease in the height of the main transition; however, the ripple phase did not vanish and the pretransition was still present in the thermograms. At the peptide concentration of 5 mol%, the metastable ripple phase disappeared without a significant change in the Tm, but the enthalpy of the main phase transition decreased by about 50% in comparison with the control. Moreover, at this concentration an additional very broad and high peak was detected at 38.8 °C with a shoulder at 36 °C. At 10 mol% ΔM3 the height of DMPG main transition peak decreased with a parallel increase in the high temperature signal. Such behavior can be interpreted in terms of phase separation, presumably into peptide-rich and peptide-poor domains. Thermodynamic parameters of the pretransition and main phase transition of DMPC/ΔM3 and DMPG/ΔM3 mixtures determined from heating and cooling scans are presented in Tables 1 and 2, respectively.

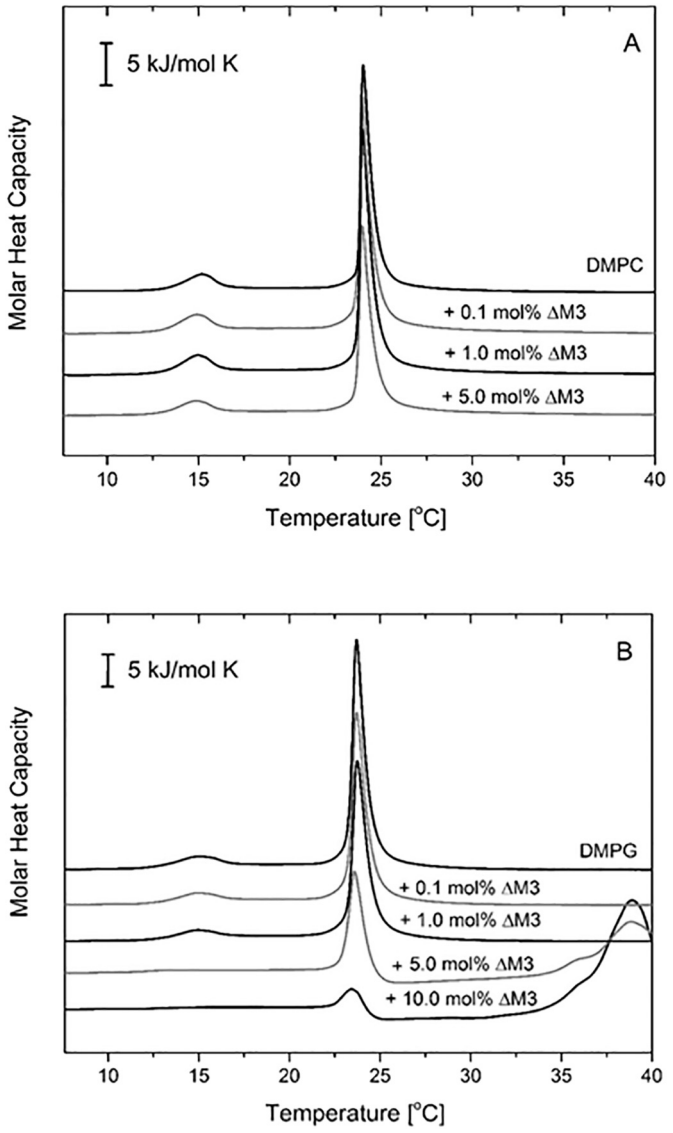

Fig. 5. Representative thermograms obtained for multilamellar A) DMPC and B) DMPG liposomes containing different concentrations of ΔM3. The enthalpy ΔH was obtained by peak integration.

3.6. Scanning electron microscopy (SEM) observations of human erythrocytes

The effects of the in vitro incubation of ΔM3 with human erythrocytes in a range of concentrations (5 to 20 μM) were monitored by SEM and are represented in Fig. 6. Under physiological conditions, normal human red blood cells assume a flattened biconcave disc shape (discocyte) of approximately 8 μm diameter (Fig. 6A). As it can be observed, when the erythrocytes were incubated with 5 μM ΔM3, equivalent to the MIC, the peptide induced a change in the normal shape in some of the erythrocytes. In fact, cells showed invaginated or cupped forms known as stomatocytes stage I. With increasing ΔM3 concentrations the effect was more evident as in addition to stomatocytes stage I, a cup-shape form with evagination of one surface and a deep invagination of the opposite face (stomatocytes stage II), and elliptic shape alterations were visible [28,29]; however, in these SEM experiments the peptide concentrations were four times higher than MIC.

4. Discussion

The incidence of *S. aureus* has significantly increased during the past few decades and it has become a leading cause of infections; ranging from minor skin and wound infections to life threatening sepsis [30–32]. One of the main clinical concerns has been the limitation of effective antimicrobial therapies given the continued emergences of the antibiotic resistant *S. aureus* strains. An attempt to develop alternative treatments has led to the evaluation of α-cAMPs from both natural and synthetic sources. In the present study, the biological activity of the synthetic novel peptide ΔM3 against *S. aureus* was investigated. The experimental results showed that ΔM3 is a potential antimicrobial agent against the susceptible ATCC 25923 and MRSA, with an MIC in the same μM range as vancomycin. Although there were no significant differences in the activity of the peptide against the two strains, this should be related with the mechanism by which ΔM3 exerts its biological activity. MRSA carries a mobile genetic element called staphylococcal cassette chromosome (SCC). This harbors the mecA gene which encodes PBP2a, a protein with low affinity for β-lactam antibiotics conferring resistance to methicillin, nafcillin, oxacillin, and cephalosporins [33,34]. Considering that the α-cAMP's mechanism of action is based on its interaction with membrane lipids and not with a specific membrane protein target, the resistant mechanism present in MRSA would not necessarily affect the activity of ΔM3. It has been previously reported that the activity of daptomycin is not affected by the resistant-mechanism present in *S. aureus* [35,36]. Daptomycin, a 13-residue lipopeptide is a particularly noteworthy antibiotic because its antibacterial activity results from direct action on membranes inducing permeabilization and depolarization [37,38]. Some of these studies demonstrated that the lipophilic acyl tail of daptomycin inserts into the cytoplasmic membrane of the

Table 1
Thermodynamic parameters of the pretransition and main phase transition of pure, fully hydrated DMPC multilamellar liposomes and DMPC/ΔM3 mixtures determined from heating and cooling scans collected at a heating (cooling) rate of 1 °C min^{-1}.

Compound	Heating						Cooling					
	Pretransition			Main transition			Pretransition			Main transition		
	ΔH [kJ mol^{-1}]	ΔS [kJ mol^{-1} K^{-1}]	T_m [°C]	ΔH [kJ mol^{-1}]	ΔS [kJ mol^{-1} K^{-1}]	T_m [°C]	ΔH [kJ mol^{-1}]	ΔS [kJ mol^{-1} K^{-1}]	T_m [°C]	ΔH [kJ mol^{-1}]	ΔS [kJ mol^{-1} K^{-1}]	T_m [°C]
DMPC												
	4.0	0.01	15.2	23.0	0.08	24.0	1.6	0.01	9.3	21.8	0.07	23.2
+ ΔM3												
0.1 mol %	3.8	0.01	14.9	26.2	0.09	24.0	2.5	0.01	9.2	25.1	0.09	23.2
1.0 mol %	4.3	0.02	15.0	26.4	0.09	24.0	1.7	0.01	9.3	26.0	0.09	23.2
5.0 mol %	3.4	0.01	14.9	22.2	0.08	24.0	1.6	0.01	9.2	20.5	0.07	23.2

Table 2
Thermodynamic parameters of the pretransition and main phase transition of pure, fully hydrated DMPG multilamellar liposomes and DMPG/ΔM3 mixtures determined from heating and cooling scans collected at a heating (cooling) rate of 1 °C min^{-1}.

Compound	Heating						Cooling					
	Pretransition			Main transition			Pretransition			Main transition		
	ΔH [kJ mol^{-1}]	ΔS [kJ mol^{-1} K^{-1}]	T_m [°C]	ΔH [kJ mol^{-1}]	ΔS [kJ mol^{-1} K^{-1}]	T_m [°C]	ΔH [kJ mol^{-1}]	ΔS [kJ mol^{-1} K^{-1}]	T_m [°C]	ΔH [kJ mol^{-1}]	ΔS [kJ mol^{-1} K^{-1}]	T_m [°C]
DMPG												
	3.9	0.01	15.0	31.9	0.11	23.7	–	–	–	31.7	0.11	22.8
+ ΔM3												
0.1 mol %	3.5	0.01	15.0	28.8	0.10	23.7	–	–	–	28.3	0.10	22.8
1.0 mol %	3.3	0.01	14.9	29.4	0.10	23.7	–	–	–	26.0	0.09	22.8
5.0 mol %	–	–	–	15.4	0.05	23.6	–	–	–	27.8	0.09	22.8
10 mol%	–	–	–	4.5	0.02	23.5	–	–	–	45.0	0.20	24.5

bacterium leading to potassium efflux, membrane depolarization, and therefore cell death [39–41]. Cui et al. [42] demonstrated that the reduction of daptomycin and vancomycin susceptibility in *S. aureus* resistant strains showed a strong correlation with the increment of cell wall thickness, which act as an obstacle to their penetration. They explained that it might be hard for daptomycin, with a molecular weight over 1620 to penetrate the cell wall when it is as thick as the one detected in MRSA, including VISA [42]. Based in their results, the authors proposed that the development of new antibiotics with smaller molecular size might be a potential new way to overcome resistant *S. aureus* infections. The results of Cui et al. support our study; in fact, the antimicrobial activity of ΔM3 was not affected, particularly considering the 49% reduction in the size of the structure in comparison with the parent peptide ΔM2 [43].

It is also important to consider that the synthesis of a shorter peptide is less expensive than that of a double size structure. However, the size is not the only physicochemical property of the peptide relevant to its biological activity. Charge and hydrophobicity are also considered crucial properties that play balanced roles in modifying the activity of a peptide [44]. The net charge of α-cAMP is the sum of all ionizable groups, this being the most relevant property in its initial electrostatic interaction with the cell membranes. Most peptides with recognized biological activity present a positive charge ranging from +2 to +9 [44]. Cationicity is favorable for initial electrostatic interactions between peptides and negatively charged bacterial membrane components. In our previous study, the increase in the charge of the polar face of ΔM2 (+9) showed a substantial increase in antimicrobial activity of the peptide in comparison with the cecropin D-like peptide [13]. In the ΔM3 design most of the charged aminoacids of the N-terminal region were preserved (+8); the analysis of the helical wheel projection of the peptide shows a potential amphipathic structure with one face containing the charged aminoacids. This region might be involved in the strong initial electrostatic interactions between the peptide and the negatively charged groups present in the predominant phospholipid constituents of the *S. aureus* membrane such as PG and CL [45]. The presence of both lipids introduces a negative charge into the membrane surface and the lipid–protein interface providing a potential binding site for peptides.

In addition, hydrophobicity also plays an important role. This is defined as the percentage of hydrophobic aminoacids within a peptide, and it is associated with the peptide insertion into a membrane hydrocarbon core [46]. For this reason, the structural modifications performed to obtain ΔM3 were focused on maintaining a hydrophobicity of 45%, the same of the parent peptide ΔM2. Peptides with high hydrophobic values present higher hemolytic activity [47]. Indeed, several studies, including those of Kiyota et al. [48] and Mor et al. [49] have found a positive correlation between the hydropathic index of peptides and their hemolytic potential. Although electrostatic interactions determine the initial attraction zwitterionic phospholipids such as those present in the outer leaflet of the erythrocyte membrane favor hydrophobic interactions by allowing the insertion of the peptide and consequently cell lysis [46].

A fundamental condition for ΔM3 as a potential systemic antibiotic is to present a minimum toxicity against cells such as erythrocytes; thus, hemolysis evaluation could be considered a measure of the peptide toxicity toward higher eukaryotic cells [50]. The control used in our experiments was melittin, a cationic (+5) at neutral pH, amphipathic, 26-amino acid with a hydrophobicity of 50%, which presents a recognized cytolytic activity at 5 μM. The results observed for ΔM3, with a charge of +8 and hydrophobicity of 45%, showed to be an active

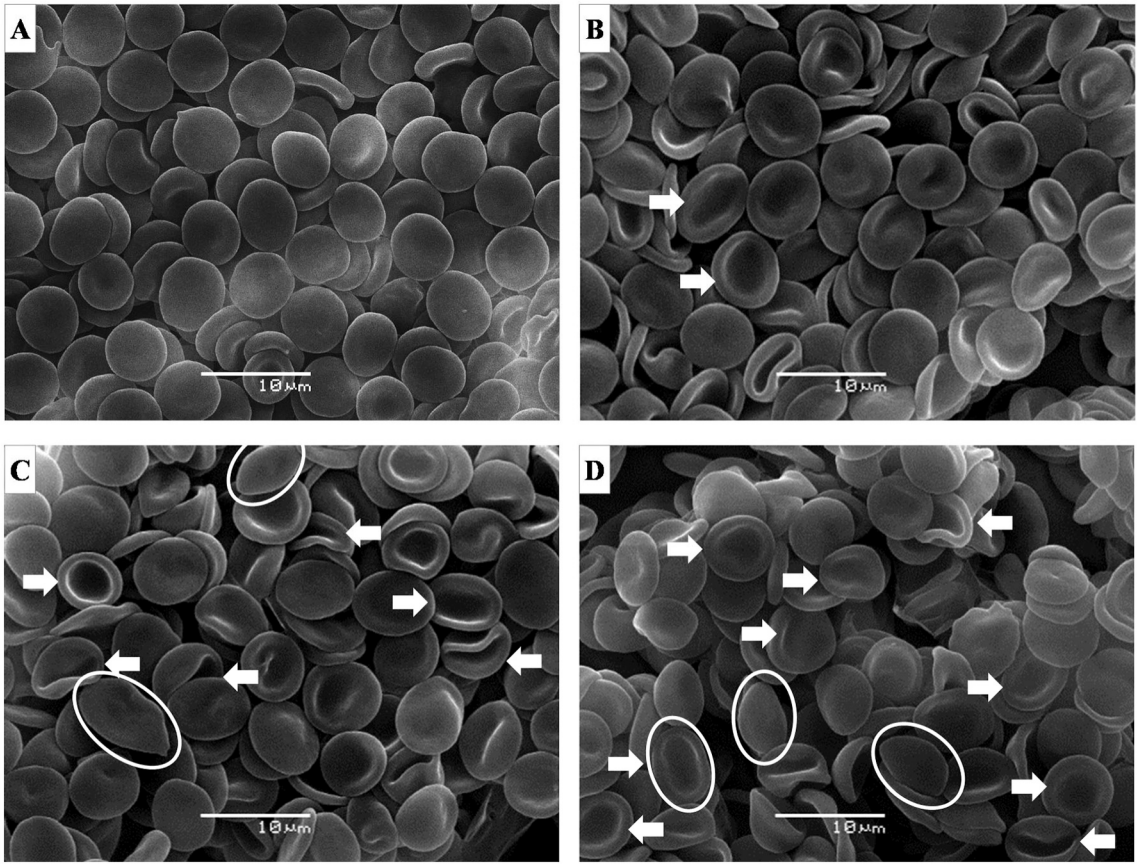

Fig. 6. Morphological changes induced on human erythrocytes by incubation with ΔM3. Images were obtained by scanning electron microscopy (SEM) of A) control, B) 5 μM, C) 10 μM and D) 20 μM ΔM3. The direction of the arrows indicate the stomatocytes stage I (to the right), stomatocytes stage II (to the left) and the circle the elliptical shape alterations.

antimicrobial agent against susceptible and MRSA strains, with an MIC in the same range as vancomycin. The hemolysis results showed that ΔM3 is slightly more hemolytic compared with the parent peptide ΔM2. This could be explained by the hydrophobicity and size of the peptides. Both are equally hydrophobic but the double size of ΔM2 could make it more difficult its insertion into the membrane. Energetically, ΔM3 might insert easily in the bilayer and therefore induce a higher hemolytic effect. However, the hemolytic effect was only evident at 4 or 5 times higher concentrations than MIC; for this reason ΔM3 might not be considered cytotoxic against human erythrocytes.

α-cAMPs with antibacterial activity are usually associated with a membrane-permeabilizing mechanism. To confirm that the biological activity of ΔM3 could be associated with this disrupting mechanism, liposomes composed of POPG and POPG:CL with an 80:20 lipid ratio were loaded with calcein; this ratio was selected in accordance to previous reports of the *S. aureus* membrane lipid composition [23,25,26]. This binary mixture reflects a more representative composition of bacterial membrane in comparison with pure POPG liposomes. If the peptide induced a lytic effect on the liposomes, the dye would be released into the external medium increasing the fluorescence. In fact, the entrapped dye shows very low fluorescence due to the self-quenching effect [19]. In a previous work, we demonstrated that the ability of ΔM2 to induce leakage in liposomes was greatly altered by the presence of CL [23]. Results of ΔM3 indicated that cardiolipin (CL) in the POPG: CL system had the ability to counteract the disrupting effect of the peptide, effect that can be explained by the structural characteristics of CL. This molecule has a conical shape with a smaller polar head group than that of POPG; the presence of cardiolipin changes the lipid packing arrangement of the liposomes in comparison with that of pure POPG due to the increase in the lateral density of fatty acids. The energetic cost of deforming a membrane with structural restrictions caused by the presence of CL is higher than the non-restricted bilayer only composed by POPG. The presence of CL induces a negative intrinsic curvature of the membrane; this structural restriction increases the free-energy cost of peptide insertion [51]. It has been suggested that this effect explains the increased resistance of the bacteria to daptomycin, which is inhibited by the increased CL content in *S. aureus* [52]. Mishra et al. [53] have performed several analyses to establish how cell membrane characteristics, including fluidity, phospholipid content and asymmetry as well as the relative surface charge play an important role in clinical daptomycin-resistant *Staphylococcus aureus* strains. The results obtained through the calcein leakage effect proved the membrane-disrupting effect of ΔM3 in POPG and also POPG:CL liposomes. These results can also be related to the antimicrobial activity of the peptide when the MICs of 5 μM and 7.5 μM were reached for the *S. aureus* ATCC 25923 and MRSA, respectively. Regarding the results obtained by Cui et al. [43], the slightly high MIC of ΔM3 against MRSA could be related to a different lipid composition in the resistant strain, making necessary more concentration of the peptide to reach the MIC. However, further studies regarding the membrane composition are needed in order to probe this hypothesis.

The X-ray results showed that ΔM3 affected the bilayer structures of both DMPC and DMPE, although to a higher extent to DMPC. The chemical difference between DMPC and DMPE is centered on their terminal amino groups, these being $-N(CH_3)_3^+$ in DMPC and $-NH_3^+$ in DMPE. Under hydrated conditions, DMPC $-N(CH_3)_3^+$ group induces the formation of a clathrate-like hydration shell around the head groups; the gradual hydration leads to water filling the highly polar inter bilayer spaces increasing their separation. This condition promotes the incorporation of the peptide molecules and the resulting structural

perturbation. On the other hand, DMPE molecules pack tighter than DMPC due to their small head groups and resultant higher effective charge [24]. Consequently, strong direct intermolecular hydrogen bonds are formed in DMPE neighboring molecules between the opposite $-NH_3^+$ and PO_4^- groups, and water molecules. Molecular details of PC and PE fully hydrated gel phases have been reported elsewhere [27,54]. The X-ray diffraction and DSC results showed that the preference for negatively charged lipids is in accordance with our previous results obtained in the calcein leakage experiments, where ΔM3 was active inducing a disruptive effect on POPG and also POPG:CL liposomes. The affinity of ΔM3 for the charged lipids explains the antimicrobial activity on *S. aureus* and the low hemolytic activity against human erythrocytes.

A commonly used membrane for studying drug-membrane interactions is that of human red blood cells. The reason for this is based on the fact that exogenous molecules induce cell-shape transformations of normal erythrocytes, which are caused by changes in the surface area of the monolayers [55]. According to the bilayer-couple hypothesis of Sheetz and Singer [56], the two halves of the erythrocyte membrane bilayer respond differently to drug induced perturbations due to the asymmetric distribution of proteins and phospholipids. Thus, any effect that expands the outer leaflet relative to the inner one produces convex structures on the cell surface (echinocytes); conversely, an expansion of the inner leaflet relative to the outer one favors concavities (stomatocytes) [57]. The results obtained by our SEM experiments indicated that ΔM3 is behaving as a mild cup-former and therefore interacts with the inner monolayer of the erythrocyte membrane, which is rich in phosphatidylethanolamines (zwitterionic) and phosphatidylserines (negatively charged).

There are several accepted models to explain the mechanism of action of cAMPs, such as the barrel-stave or carpet models [58]. However, most of them establish that the first step is based on a binding process mediated by electrostatic interactions between the cationic residues of the peptide and the anionic lipids of the membrane target. The X- ray diffraction and DSC results evidence the different kind of interaction of ΔM3 with charged than with zwitterionic phospholipids. These results are important because the preference of ΔM3 for negatively charged lipids may be associated with the selectivity to lyse bacterial membranes rather than eukaryotic membranes. Low-affinity to zwitterionic lipids compared with charged lipids constitute a key for the rationale design of novel and more selective peptide-based antibiotics. The results obtained with ΔM3, a substantially (49%) downsized analogue of ΔM2 demonstrate its potential against resistant strains of *S. aureus*. Additionally, our results constitute a useful approach to the identification of the minimal active region of bioactive peptides, which may contribute to reducing the production cost of a pharmaceutical agent.

Declaration of competing interest

The authors declare that they have no competing, financial, or personal relationships that could influence the work reported in this paper.

Acknowledgements

This work was supported by the University of Antioquia (CODI Grant 2015-7669) and COLCIENCIAS (Grant 120465843150, RC-611-2014). This work was financially supported in part by the statutory funds of the Faculty of Biochemistry, Biophysics and Biotechnology, Jagiellonian University. DSC measurements were carried out using the instrument purchased thanks to financial support from the European Regional Development Fund (contract No. POIG.02.01.00-12-167/08, Project Malopolska Centre of Biotechnology).

Appendix A. Supplementary data

Supplementary data to this article can be found online at https://doi.org/10.1016/j.bbamem.2020.183498.

References

[1] M. Mahlapuu, J. Håkansson, L. Ringstad, C. Björn, Antimicrobial peptides: an emerging category of therapeutic agents, Front. Cell. Infect. Mi. 6 (2016).
[2] E.F. Haney, S.K. Straus, R.E. Hancock, Reassessing the host defense peptide landscape, Front. Chem. 7 (2019) 43.
[3] V.N. Lazarev, V.M. Govorun, Antimicrobial peptides and their use in medicine, Appl. Biochem. Microbiol. 46 (2010) 803–814.
[4] S.Y. Tong, J.S. Davis, E. Eichenberger, T.L. Holland, V.G. Fowler, Staphylococcus aureus infections: epidemiology, pathophysiology, clinical manifestations, and management, Clin. Microbiol. Rev. 28 (2015) 603–661.
[5] H.F. Wertheim, D.C. Melles, M.C. Vos, W. van Leeuwen, A. van Belkum, H. A. Verbrugh, J.L. Nouwen, The role of nasal carriage in Staphylococcus aureus infections, Lancet Infect. Dis. 5 (2005) 751–762.
[6] C.-J. Kim, H.-B. Kim, M.-d. Oh, Y. Kim, A. Kim, S.-H. Oh, K.-H. Song, E.S. Kim, Y. K. Cho, Y.H. Choi, The burden of nosocomial staphylococcus aureus bloodstream infection in South Korea: a prospective hospital-based nationwide study, BMC Infect. Dis. 14 (2014) 590.
[7] R.L. Thompson, I. Cabezudo, R.P. Wenzel, Epidemiology of nosocomial infections caused by methicillin-resistant Staphylococcus aureus, Ann. Intern. Med. 97 (1982) 309–317.
[8] S. Hiraoka, H. Matsuzaki, I. Shibuya, Active increase in cardiolipin synthesis in the stationary growth phase and its physiological significance in Escherichia coli, FEBS Lett. 336 (1993) 221–224.
[9] F.L. Hoch, Cardiolipins and biomembrane function, Biochim. Biophys. Acta Biomembr. 1113 (1992) 71–133.
[10] S.A. Short, D.C. White, Biosynthesis of cardiolipin from phosphatidylglycerol in Staphylococcus aureus, J. Bacteriol. 109 (1972) 820–826.
[11] M. Tsai, R.L. Ohniwa, Y. Kato, S.L. Takeshita, T. Ohta, S. Saito, H. Hayashi, K. Morikawa, Staphylococcus aureus requires cardiolipin for survival under conditions of high salinity, BMC Microbiol. 11 (2011) 13.
[12] M. Cytryńska, P. Mak, A. Zdybicka-Barabas, P. Suder, T. Jakubowicz, Purification and characterization of eight peptides from galleria mellonella immune hemolymph, Peptides 28 (2007) 533–546.
[13] J. Oñate-Garzón, A. Ausili, M. Manrique-Moreno, A. Torrecillas, F.J. Aranda, E. Patiño, J.C. Gomez-Fernández, The increase in positively charged residues in cecropin D-like Galleria mellonella favors its interaction with membrane models that imitate bacterial membranes, Arch. Biochem. Biophys. 629 (2017) 54–62.
[14] M. Pate, J. Blazyk, Methods for assessing the structure and function of cationic antimicrobial peptides, in: W.S. Champney (Ed.), New Antibiotic Targets, Humana Press, 2008, pp. 155–173.
[15] W.L. DeLano, The PyMOL molecular graphics system. http://www.pymol.org, 2002.
[16] I. Wiegand, K. Hilpert, R.E. Hancock, Agar and broth dilution methods to determine the minimal inhibitory concentration (MIC) of antimicrobial substances, Nat. Protoc. 3 (2008) 163–175.
[17] B.L. Spaller, J.M. Trieu, P.F. Almeida, Hemolytic activity of membrane-active peptides correlates with the thermodynamics of binding to 1-palmitoyl-2-oleoyl-sn-glycero-3-phosphocholine bilayers, J. Memb.Biol. 246 (2013) 257–262.
[18] A. Oddo, P.R. Hansen, Hemolytic activity of antimicrobial peptides, in: Antimicrobial Peptides, Springer, 2017, pp. 427–435.
[19] B. Maherani, E. Arab-Tehrany, A. Kheirolomoom, D. Geny, M. Linder, Calcein release behavior from liposomal bilayer; influence of physicochemical/mechanical/structural properties of lipids, Biochimie 95 (2013) 2018–2033.
[20] E.F. Haney, S.C. Mansour, R.E. Hancock, Antimicrobial peptides: an introduction, in: Antimicrobial Peptides, Springer, 2017, pp. 3–22.
[21] P. Wayne, Clinical and Laboratory Standards Institute (CLSI); 2010, Performance Standards for Antimicrobial Susceptibility Testing 20, 2010.
[22] G. Van Den Bogaart, J.V. Guzmán, J.T. Mika, B. Poolman, On the mechanism of pore formation by melittin, J. Biol. Chem. 283 (2008) 33854–33857.
[23] L. Hernández-Villa, M. Manrique-Moreno, C. Leidy, M. Jemioła-Rzemińska, C. Ortíz, K. Strzałka, Biophysical evaluation of cardiolipin content as a regulator of the membrane lytic effect of antimicrobial peptides, Biophys. Chem. 238 (2018) 8–15.
[24] M. Suwalsky, Phospholipid bilayers, in: J.C. Salamone (Ed.), Polymeric Materials Encyclopedia vol. 7, CRC Press, Boca Raton, 1996, pp. 5073–5078.
[25] M.I. Perez, S.M. Trier, A. Bernal, J.C. Vargas, C. Herrfurth, I. Feussner, J. M. Gonzalez, C. Leidy, S. Aureus adapt to growth conditions by changing membrane order, Biophys. J. 106 (2014) 580a.
[26] D.C. White, F.E. Frerman, Extraction, characterization, and cellular localization of the lipids of Staphylococcus aureus, J. Bacteriol. 94 (1967) 1854–1867.
[27] S. Tristram-Nagle, Y. Liu, J. Legleiter, J.F. Nagle, Structure of gel phase DMPC determined by X-Ray diffraction, Biophys. J. 83 (2002) 3324–3335.
[28] H.W.G. Lim, M. Wortis, R. Mukhopadhyay, Soft Matter, WILEY-VCH Verlag GmbH & Co. KGaA, Weinheim, 2008.
[29] H.W.G. Lim, M. Wortis, R. Mukhopadhyay, Red blood cell shapes and shape transformations: Newtonian mechanicsof a composite membrane, in: G. Gompper, M. Schick (Eds.), Soft Matter vol. 4, WILEY-VCH Verlag GmbH & Co. KGaA, Weinheim, 2008, pp. 83–202.
[30] E.J. Gorak, S.M. Yamada, J.D. Brown, Community-acquired methicillin-resistant Staphylococcus aureus in hospitalized adults and children without known risk factors, Clin. Infect. Dis. 29 (1999) 797–800.
[31] R.M. Klevens, M.A. Morrison, J. Nadle, S. Petit, K. Gershman, S. Ray, L.H. Harrison, R. Lynfield, G. Dumyati, J.M. Townes, Invasive methicillin-resistant Staphylococcus aureus infections in the United States, JAMA 298 (2007) 1763–1771.

[32] F.D. Lowy, Staphylococcus aureus infections, N. Engl. J. Med. 339 (1998) 520–532.
[33] T.J. Foster, J.A. Geoghegan, Chapter 37 - Staphylococcus aureus, in: Y.-W. Tang, M. Sussman, D. Liu, I. Poxton, J. Schwartzman (Eds.), Molecular Medical Microbiology, Second edition, Academic Press, Boston, 2015, pp. 655–674.
[34] S.M. Opal, A. Pop-Vicas, Molecular mechanisms of antibiotic resistance in bacteria, in: J.E. Bennett, R. Dolin, M.J. Blaser (Eds.), Mandell, Douglas, and Bennett's Principles and Practice of Infectious Diseases, ELSEVIER, Philadelphia, 2015, pp. 235–251.
[35] B.M. Diederen, I. van Duijn, P. Willemse, J.A. Kluytmans, In vitro activity of daptomycin against methicillin-resistant Staphylococcus aureus, including heterogeneously glycopeptide-resistant strains, Antimicrob. Agents Chemother. 50 (2006) 3189–3191.
[36] J.J. Picazo, C. Betriu, I. Rodríguez-Avial, E. Culebras, F. Lopez, M. Gomez, Comparative activity of daptomycin against clinical isolates of methicillin-resistant Staphylococcus aureus and coagulase-negative staphylococci, Enferm. Infecc. Microbiol. Clin. 28 (2009) 13–16.
[37] J.A. Silverman, N.G. Perlmutter, H.M. Shapiro, Correlation of daptomycin bactericidal activity and membrane depolarization in Staphylococcus aureus, Antimicrob. Agents Chemother. 47 (2003) 2538–2544.
[38] J.K. Hobbs, K. Miller, A.J. O'neill, I. Chopra, Consequences of daptomycin-mediated membrane damage in Staphylococcus aureus, J. Antimicrob. Chemother. 62 (2008) 1003–1008.
[39] N. Cotroneo, R. Harris, N. Perlmutter, T. Beveridge, J.A. Silverman, Daptomycin exerts bactericidal activity without lysis of Staphylococcus aureus, Antimicrob. Agents Chemother. 52 (2008) 2223–2225.
[40] Y.-h. Xing, W. Wang, S.-q. Dai, T.-y. Liu, J.-j. Tan, G.-l. Qu, Y.-x. Li, Y. Ling, G. Liu, X.-q. Fu, Daptomycin exerts rapid bactericidal activity against bacillus anthracis without disrupting membrane integrity, Acta Pharmacol. Sin. 35 (2014) 211–218.
[41] W.R. Miller, A.S. Bayer, C.A. Arias, Mechanism of action and resistance to daptomycin in Staphylococcus aureus and enterococci, Cold Spring Harb. Perspect. Med. 6 (2016) a026997.
[42] L. Cui, E. Tominaga, H.-m. Neoh, K. Hiramatsu, Correlation between reduced daptomycin susceptibility and vancomycin resistance in vancomycin-intermediate Staphylococcus aureus, Antimicrob. Agents Chemother. 50 (2006) 1079–1082.
[43] J. Oñate-Garzón, M. Manrique-Moreno, S. Trier, C. Lady, R. Torres, E. Patiño, Antimicrobial activity and interactions of cationic peptides derived from galleria mellonella cecropin D-like peptide with model membranes, J. Antibiot. 70 (2017) 238–245.
[44] L.M. Yin, M.A. Edwards, J. Li, C.M. Yip, C.M. Deber, Roles of hydrophobicity and charge distribution of cationic antimicrobial peptides in peptide-membrane interactions, J. Biol. Chem. 287 (2012) 7738–7745.
[45] M. Schlame, Thematic review series: Glycerolipids. Cardiolipin synthesis for the assembly of bacterial and mitochondrial membranes, J. Lipid Res. 49 (2008) 1607–1620.
[46] Y. Chen, M.T. Guarnieri, A.I. Vasil, M.L. Vasil, C.T. Mant, R.S. Hodges, Role of peptide hydrophobicity in the mechanism of action of α-helical antimicrobial peptides, Antimicrob. Agents Chemother. 51 (2007) 1398–1406.
[47] T. Wieprecht, M. Dathe, M. Beyermann, E. Krause, W.L. Maloy, D.L. MacDonald, M. Bienert, Peptide hydrophobicity controls the activity and selectivity of magainin 2 amide in interaction with membranes, Biochemistry (Mosc) 36 (1997) 6124–6132.
[48] T. Kiyota, S. Lee, G. Sugihara, Design and synthesis of Amphiphilic α-helical model peptides with systematically varied hydrophobic– hydrophilic balance and their interaction with lipid-and bio-membranes, Biochemistry (Mosc) 35 (1996) 13196–13204.
[49] A. Mor, K. Hani, P. Nicolas, The vertebrate peptide antibiotics dermaseptins have overlapping structural features but target specific microorganisms, J. Biol. Chem. 269 (1994) 31635–31641.
[50] K. Fosgerau, T. Hoffmann, Peptide therapeutics: current status and future directions, Drug Discov. Today 20 (2015) 122–128.
[51] D. Koller, K. Lohner, The role of spontaneous lipid curvature in the interaction of interfacially active peptides with membranes, Biochim. Biophys. Acta Biomembr. 1838 (2014) 2250–2259.
[52] T. Zhang, J.K. Muraih, N. Tishbi, J. Herskowitz, R.L. Victor, J. Silverman, S. Uwumarenogie, S.D. Taylor, M. Palmer, E. Mintzer, Cardiolipin prevents membrane translocation and permeabilization by daptomycin, J. Biol. Chem. 289 (2014) 11584–11591.
[53] N.N. Mishra, S.-J. Yang, A. Sawa, A. Rubio, C.C. Nast, M.R. Yeaman, A.S. Bayer, Analysis of cell membrane characteristics of in vitro-selected daptomycin-resistant strains of methicillin-resistant Staphylococcus aureus, Antimicrob. Agents Chemother. 53 (2009) 2312–2318.
[54] J. Katsaras, S. Tristram-Nagle, Y. Liu, R. Headrick, E. Fontes, P. Mason, J.F. Nagle, Clarification of the ripple phase of lecithin bilayers using fully hydrated, aligned samples, Phys. Rev. E 61 (2000) 5668.
[55] A. Iglic, V. Kralj-Iglic, H. Hägerstrand, Amphiphile induced echinocyte-spheroechinocyte transformation of red blood cell shape, Eur. Biophys. J. 27 (1998) 335–339.
[56] M.P. Sheetz, S.J. Singer, Biological membranes as bilayer couples. A molecular mechanism of drug-erythrocytes interactions, Proc. Natl. Acad. Sci. U. S. A. 71 (1974) 4457–4461.
[57] K.D. Tachev, K.D. Danov, P.A. Kralchevsky, On the mechanism of stomatocyte-echinocyte transformations of red blood cells: experiment and theoretical model, Colloids Surf., B 34 (2004) 123–140.
[58] M. Zasloff, Antimicrobial peptides of multicellular organisms, Nature 415 (2002) 389–395.